Immunity, Volume *53*

Supplemental Information

SARS-CoV-2 mRNA Vaccines Foster Potent Antigen-Specific Germinal Center Responses Associated with Neutralizing Antibody Generation

Katlyn Lederer, Diana Castaño, Daniela Gómez Atria, Thomas H. Oguin III, Sidney Wang, Tomaz B. Manzoni, Hiromi Muramatsu, Michael J. Hogan, Fatima Amanat, Patrick Cherubin, Kendall A. Lundgreen, Ying K. Tam, Steven H.Y. Fan, Laurence C. Eisenlohr, Ivan Maillard, Drew Weissman, Paul Bates, Florian Krammer, Gregory D. Sempowski, Norbert Pardi, and Michela Locci

Figure S1

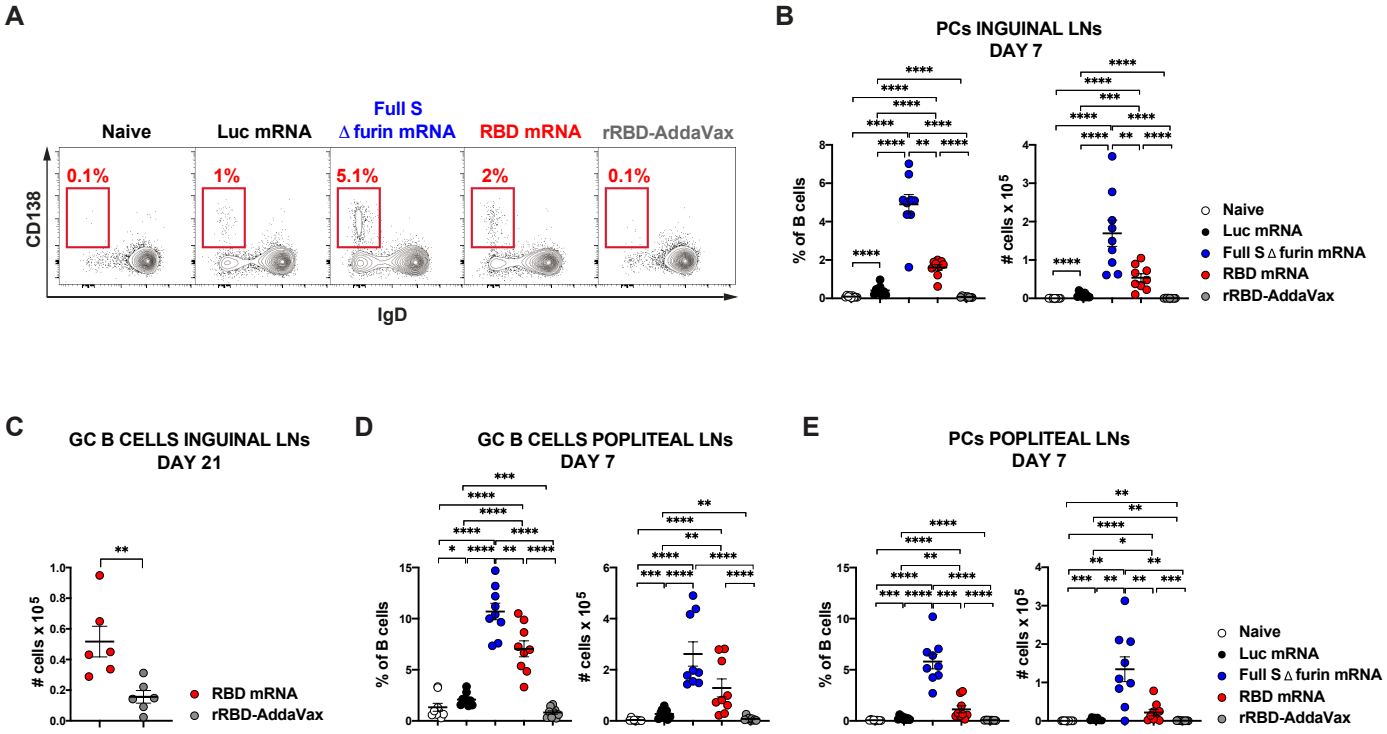
A
Naive
Luc mRNA
Full S
Δ furin mRNA
RBD mRNA
rRBD-AddaVax
0.1%
1%
5.1%
2%
0.1%
CD138
IgD
B
PCs INGUINAL LNs
DAY 7
% of B cells
# cells x 10^5
Naive
Luc mRNA
Full S Δ furin mRNA
RBD mRNA
rRBD-AddaVax
C
GC B CELLS INGUINAL LNs
DAY 21
cells x 10^5
RBD mRNA
rRBD-AddaVax
D
GC B CELLS POPLITEAL LNs
DAY 7
% of B cells
# cells x 10^5
E
PCs POPLITEAL LNs
DAY 7
% of B cells
# cells x 10^5
Naive
Luc mRNA
Full S Δ furin mRNA
RBD mRNA
rRBD-AddaVax

Figure S2

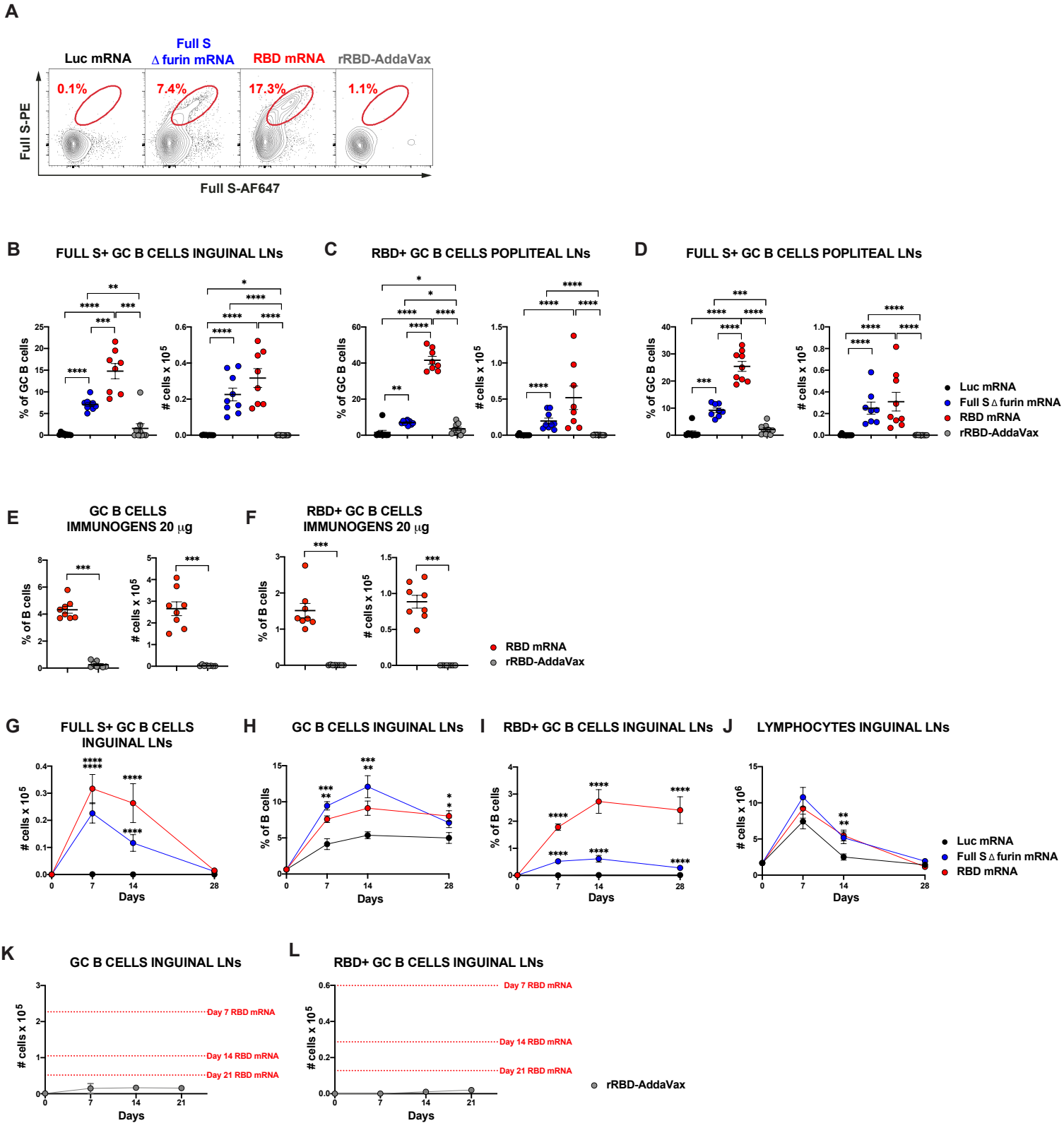
A
Luc mRNA
Full S Δ furin mRNA
RBD mRNA
rRBD-AddaVax
0.1%
7.4%
17.3%
1.1%
Full S-PE
Full S-AF647
B
FULL S+ GC B CELLS INGUINAL LNs
% of GC B cells
# cells x 10^5
C
RBD+ GC B CELLS POPLITEAL LNs
D
FULL S+ GC B CELLS POPLITEAL LNs
Luc mRNA
Full S Δ furin mRNA
RBD mRNA
rRBD-AddaVax
E
GC B CELLS IMMUNOGENS 20 μg
% of B cells
F
RBD+ GC B CELLS IMMUNOGENS 20 μg
RBD mRNA
rRBD-AddaVax
G
FULL S+ GC B CELLS INGUINAL LNs
Days
H
GC B CELLS INGUINAL LNs
I
RBD+ GC B CELLS INGUINAL LNs
J
LYMPHOCYTES INGUINAL LNs
cells x 10^6
Luc mRNA
Full S Δ furin mRNA
RBD mRNA
K
GC B CELLS INGUINAL LNs
Day 7 RBD mRNA
Day 14 RBD mRNA
Day 21 RBD mRNA
L
RBD+ GC B CELLS INGUINAL LNs
rRBD-AddaVax

Figure S3

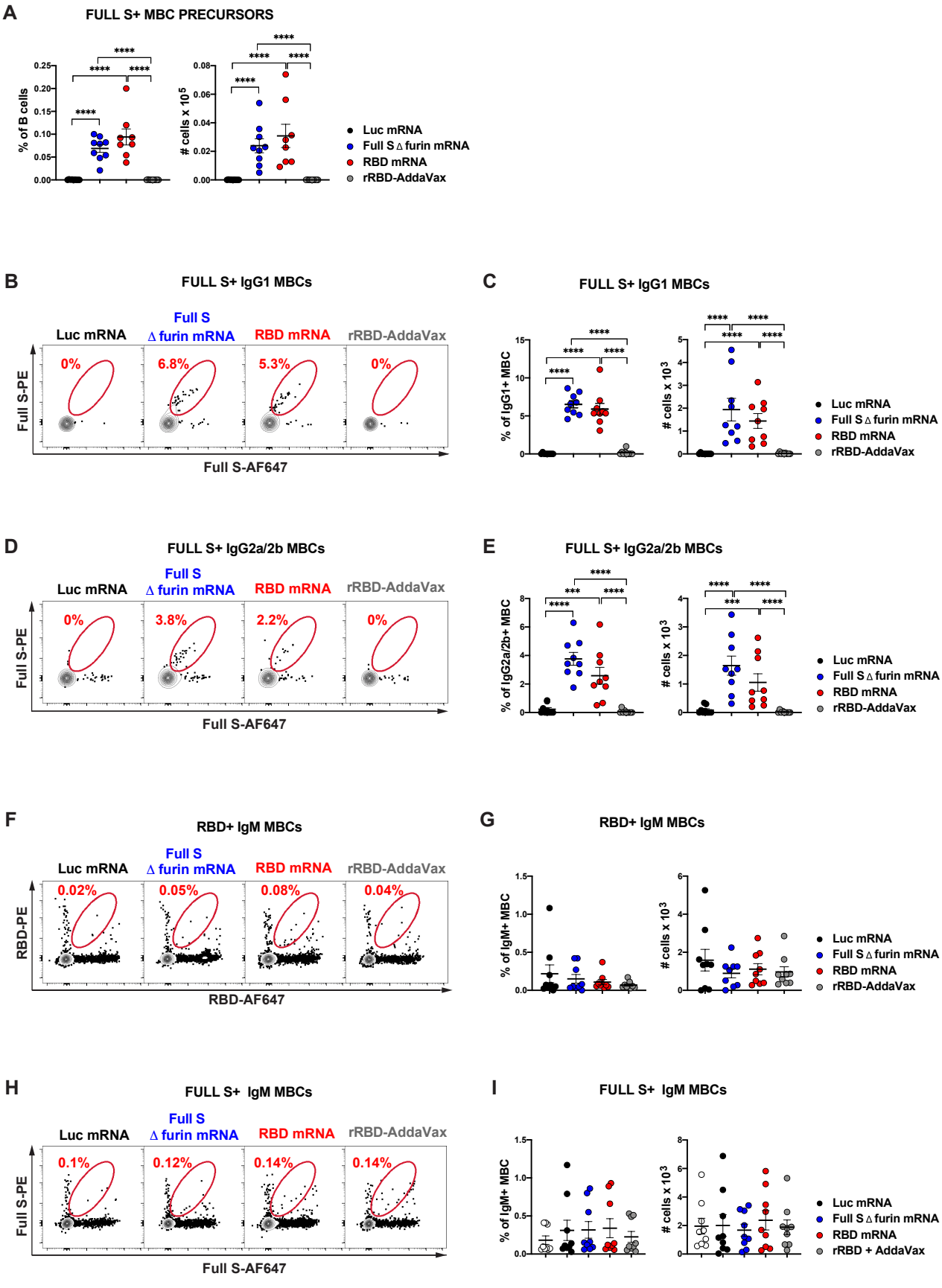
A
FULL S+ MBC PRECURSORS
% of B cells
# cells x 10^5
Luc mRNA
Full S Δ furin mRNA
RBD mRNA
rRBD-AddaVax
B
FULL S+ IgG1 MBCs
Luc mRNA
Full S Δ furin mRNA
RBD mRNA
rRBD-AddaVax
0%
6.8%
5.3%
0%
Full S-PE
Full S-AF647
C
FULL S+ IgG1 MBCs
% of IgG1+ MBC
# cells x 10^3
D
FULL S+ IgG2a/2b MBCs
0%
3.8%
2.2%
0%
E
FULL S+ IgG2a/2b MBCs
% of IgG2a/2b+ MBC
F
RBD+ IgM MBCs
0.02%
0.05%
0.08%
0.04%
RBD-PE
RBD-AF647
G
RBD+ IgM MBCs
% of IgM+ MBC
H
FULL S+ IgM MBCs
0.1%
0.12%
0.14%
0.14%
I
FULL S+ IgM MBCs
rRBD + AddaVax

Figure S4

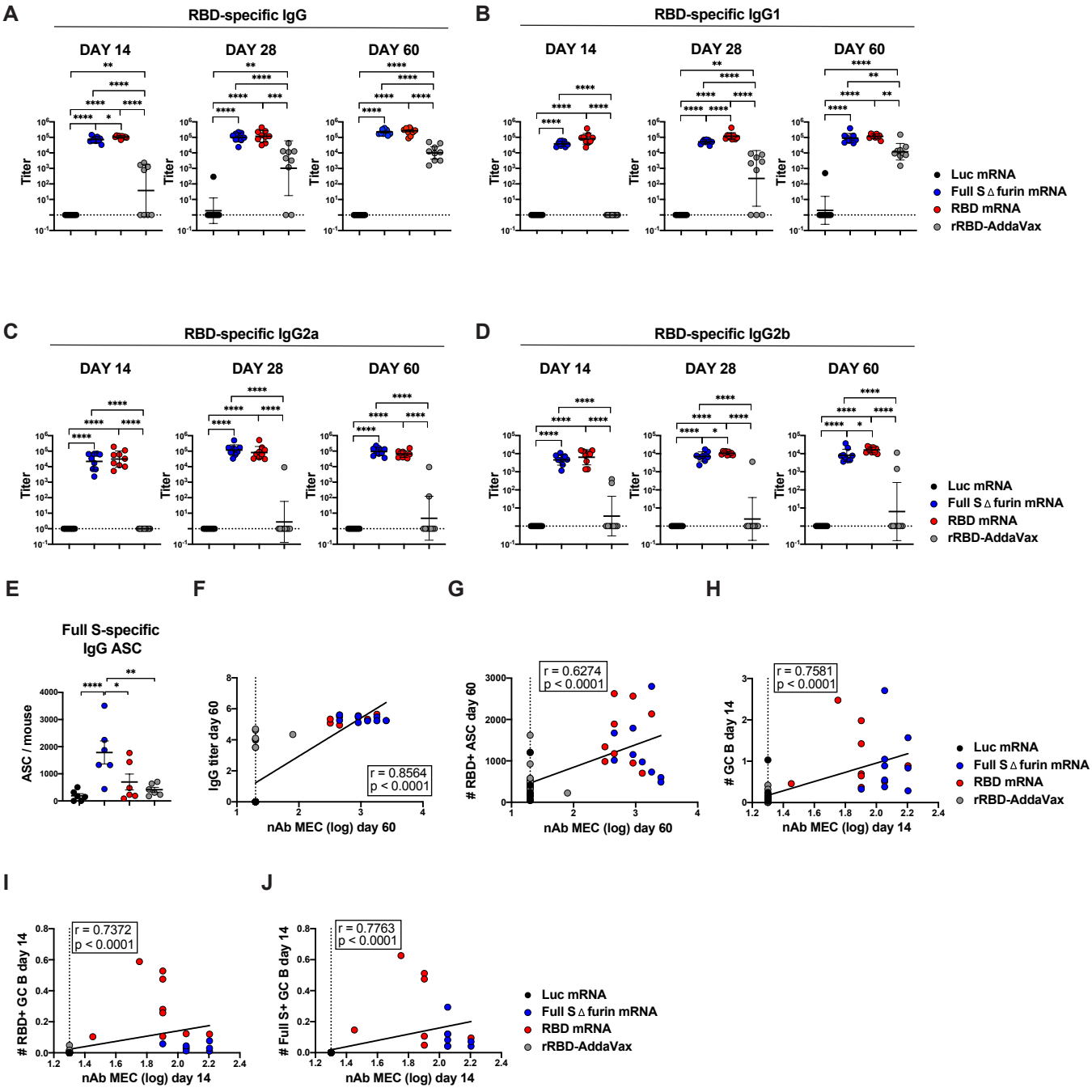
A
RBD-specific IgG
DAY 14
DAY 28
DAY 60
Titer
B
RBD-specific IgG1
C
RBD-specific IgG2a
D
RBD-specific IgG2b
Luc mRNA
Full S Δ furin mRNA
RBD mRNA
rRBD-AddaVax
E
Full S-specific IgG ASC
ASC / mouse
F
IgG titer day 60
r = 0.8564
p < 0.0001
nAb MEC (log) day 60
G
# RBD+ ASC day 60
r = 0.6274
p < 0.0001
H
# GC B day 14
r = 0.7581
p < 0.0001
nAb MEC (log) day 14
I
# RBD+ GC B day 14
r = 0.7372
p < 0.0001
J
# Full S+ GC B day 14
r = 0.7763
p < 0.0001

Figure S5

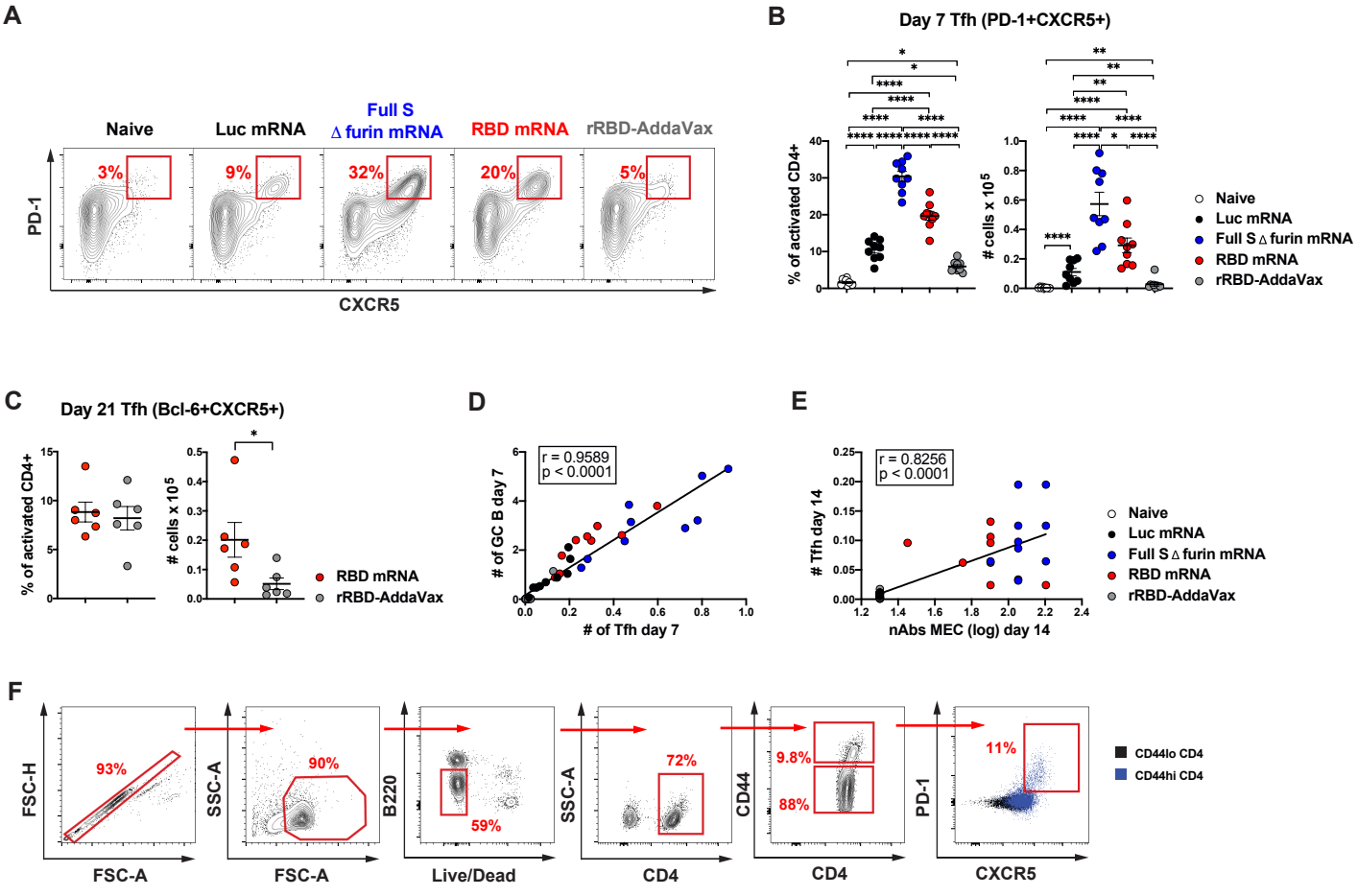
A
Naive
Luc mRNA
Full S Δ furin mRNA
RBD mRNA
rRBD-AddaVax
3%
9%
32%
20%
5%
PD-1
CXCR5
B
Day 7 Tfh (PD-1+CXCR5+)
% of activated CD4+
# cells x 10^5
Naive
Luc mRNA
Full S Δ furin mRNA
RBD mRNA
rRBD-AddaVax
C
Day 21 Tfh (Bcl-6+CXCR5+)
% of activated CD4+
# cells x 10^5
RBD mRNA
rRBD-AddaVax
D
r = 0.9589
p < 0.0001
# of GC B day 7
# of Tfh day 7
E
r = 0.8256
p < 0.0001
Tfh day 14
nAbs MEC (log) day 14
Naive
Luc mRNA
Full S Δ furin mRNA
RBD mRNA
rRBD-AddaVax
F
93%
FSC-H
FSC-A
90%
SSC-A
FSC-A
59%
B220
Live/Dead
72%
SSC-A
CD4
9.8%
88%
CD44
CD4
11%
PD-1
CXCR5
CD44lo CD4
CD44hi CD4

Figure S6

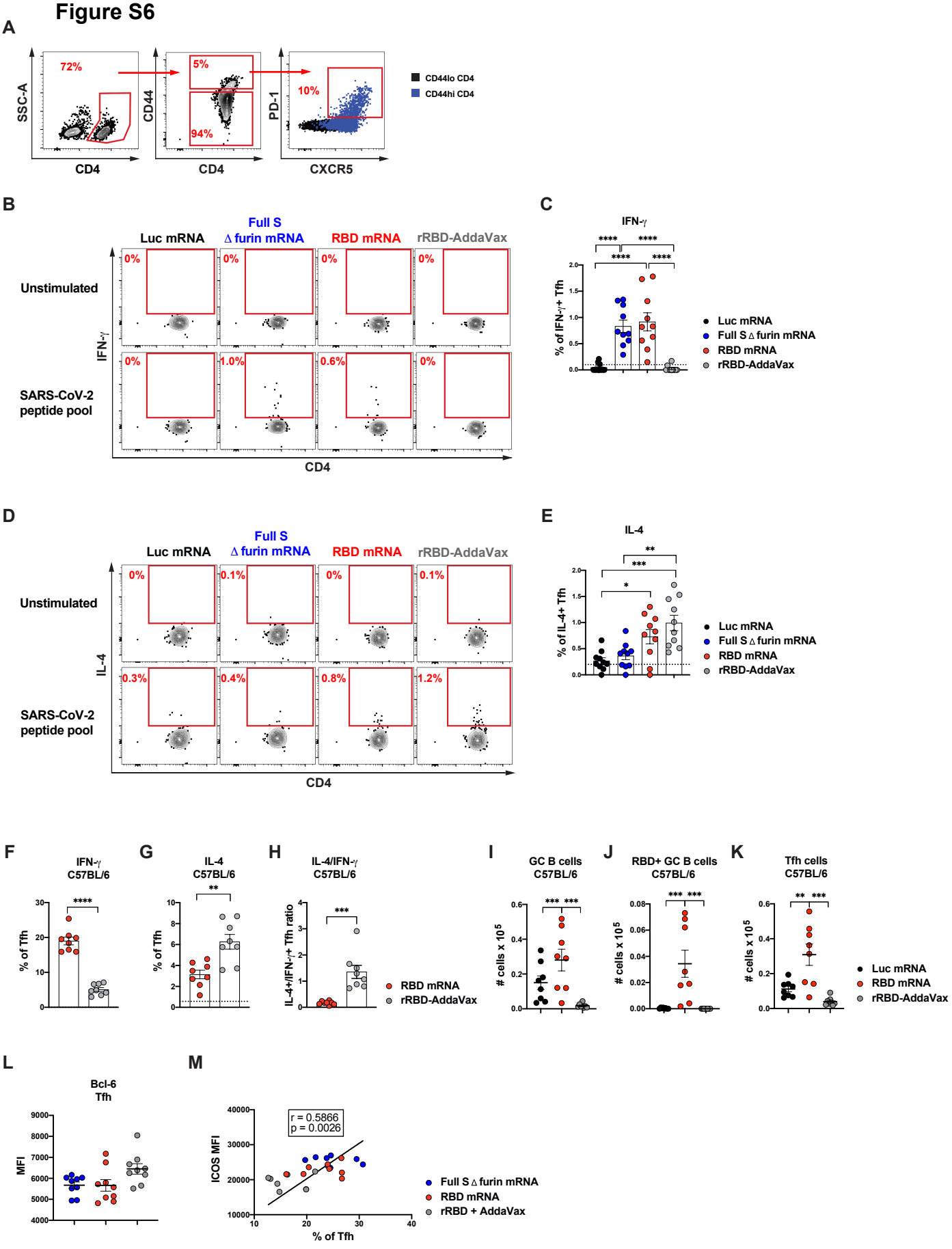
A
72%
5%
94%
10%
SSC-A
CD4
CD44
CD4
PD-1
CXCR5
CD44lo CD4
CD44hi CD4
B
Full S
Luc mRNA
Δ furin mRNA
RBD mRNA
rRBD-AddaVax
Unstimulated
SARS-CoV-2 peptide pool
IFN-γ
CD4
0%
0%
0%
0%
0%
1.0%
0.6%
0%
C
IFN-γ
% of IFN-γ+ Tfh
****
Luc mRNA
Full S Δ furin mRNA
RBD mRNA
rRBD-AddaVax
D
Full S
Luc mRNA
Δ furin mRNA
RBD mRNA
rRBD-AddaVax
Unstimulated
SARS-CoV-2 peptide pool
IL-4
CD4
0%
0.1%
0%
0.1%
0.3%
0.4%
0.8%
1.2%
E
IL-4
% of IL-4+ Tfh
**
***
*
Luc mRNA
Full S Δ furin mRNA
RBD mRNA
rRBD-AddaVax
F
IFN-γ
C57BL/6
% of Tfh
****
G
IL-4
C57BL/6
% of Tfh
**
H
IL-4/IFN-γ
C57BL/6
IL-4+/IFN-γ+ Tfh ratio
***
RBD mRNA
rRBD-AddaVax
I
GC B cells
C57BL/6
cells x 10^5
*** ***
J
RBD+ GC B cells
C57BL/6
cells x 10^5
*** ***
K
Tfh cells
C57BL/6
cells x 10^5
** ***
Luc mRNA
RBD mRNA
rRBD-AddaVax
L
Bcl-6
Tfh
MFI
M
r = 0.5866
p = 0.0026
ICOS MFI
% of Tfh
Full S Δ furin mRNA
RBD mRNA
rRBD + AddaVax

Figure S7

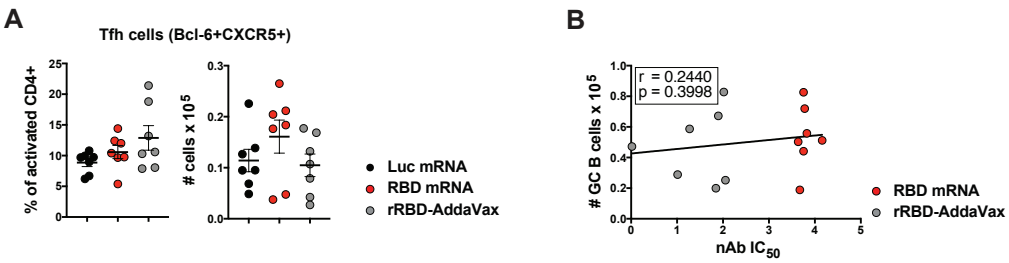
A
Tfh cells (Bcl-6+CXCR5+)
% of activated CD4+
# cells x 10^5
Luc mRNA
RBD mRNA
rRBD-AddaVax
B
r = 0.2440
p = 0.3998
# GC B cells x 10^5
nAb IC50
RBD mRNA
rRBD-AddaVax

Table S1. Flow cytometry panel for Tfh detection. Related to Figures 5 and 6.

Antibody/Conjugation	Conjugation	Dilution Factor	Clone
CD16/CD32	Purified	1:1000	2.4G2
Fixable Viability Dye	eFluor780	1:2000	n/a
B220	BV650	1:400	RA3-6B2
CXCR5	Biotin	1:50	SPRCL5
Streptavidin	BV421	1:500	n/a
CD4	PerCP-Cy5.5	1:200	RM4-5
PD-1	PE-Cy7	1:200	RMP1-30
CD44	BV605	1:400	IM7
CD62L	BUV395	1:400	MEL-14
Bcl6	AF647	1:200	K112-91
ICOS	AF488	1:400	C398.4A

Table S2. Flow cytometry panel for identification of total and antigen specific GC B cells, and antigen specific MBC precursors in LNs. Related to Figures 1, 2 and 3.

Antibody, protein or reagent	Conjugation	Dilution Factor	Clone
CD16/CD32	Purified	1:1000	2.4G2
Streptavidin	AF488	1:500	n/a
Fixable Viability	eFluor780	1:2000	n/a
CD19	BV605	1:800	6D5
FAS	BV510	1:800	Jo2
IgD	PE-Cy7	1:400	11-26c
GL7	PerCP-Cy5.5	1:400	GL7
CD3	APC-Fire750	1:400	17A2
Ter-119	APC-Fire750	1:400	Ter119
CD138	BV650	1:400	281-2
CXCR4	Biotin	1:200	2B11
CD86	BV421	1:200	GL1
CCR6	BV786	1:400	29-2L17
Recombinant RBD or full S	AF647	1:3200	n/a
Recombinant RBD or full S	PE	1:1500	n/a

Table S3. Flow cytometry panel for identification of antigen specific MBCs. Related to Figure 3.

Antibody	Conjugation	Dilution Factor	Clone
CD16/CD32 Purified	Purified	1:1000	2.4G2
Fixable Viability eFluor780	eFluor780	1:2000	n/a
CD19 BV605	BV605	1:800	6D5
FAS BV510	BV510	1:800	Jo2
CD3 APC-Fire750	APC-Fire750	1:400	17A2
Ter-119 APC-Fire750	APC-Fire750	1:400	Ter-119
B220 Alexa Fluor 700	AF700	1:400	RA3-6B2
CD38 PE-Cy7	PE-Cy7	1:400	90
IgG1 eFluor450	V450	1:400	A85-1

IgG2a/2b	BB700	1:400	R2-40
IgM	FITC	1:400	Polyclonal
IgD	BV650	1:400	11-26c
Recombinant RBD or Full Spike	AF647	1:3200	n/a
Recombinant RBD or Full Spike PE	PE	1:1500	n/a

Table S4. Flow cytometry panel for ICS experiments. Related to Figures 5 and 6.

Antibody/Conjugation	Conjugation	Dilution Factor	Clone
CD16/CD32	Purified	1:1000	2.4G2
Fixable Viability Dye	eFluor780	1:2000	n/a
CD4	PerCP-Cy5.5	1:200	RM4-5
PD-1	PE-Cy7	1:200	RMP1-30
CD44	BV605	1:400	IM7
CXCR5	BV421	1:50	L138D7
B220	AF700	1:400	RA3-6B2
IL-4	AF647	1:100	11B11
IFN-γ	BV650	1:100	XMG1.2
IL-21R FC Chimera	n/a	1:20	n/a
Anti-human IgG Fc	PE	1:50	n/a

Table S5. Panel for confocal microscopy. Related to Figure 1.

Antibody	Conjugation	Dilution Factor	Clone
CD16/CD32 Purified	Purified	1:1000	2.4G2
CD21/35	BV421	1:200	7E9
GL7	AF488	1:100	6D5
CD3	AF594	1:200	17A2
IgD	AF647	1:200	11-26c

SUPPLEMENTAL FIGURE TITLES AND LEGENDS

Figure S1. SARS-CoV-2 vaccines induce comparable B cell responses in both draining inguinal and popliteal LNs. Related to Figure 1. Mice were immunized into the gastrocnemius muscle (i.m.) with 30 μg of Luc, full S Δ furin or RBD mRNA or 10 μg recombinant RBD protein adjuvanted with AddaVax (rRBD-AddaVax). LNs were analyzed 7 or 21 days later. **(A)** Representative analysis of plasma cells (PCs): cells are gated on, live, and dump$^-$ CD19$^+$ cells from inguinal LNs at day 7. **(B)** Frequency (left) and absolute numbers (right) of PCs in inguinal LNs at day 7. **(C)** Absolute numbers of GC B cells in inguinal LNs at day 21 **(D)** Frequency (left) and absolute numbers (right) of GC B cells in popliteal LNs at day 7. **(E)** Frequency (left) and absolute numbers (right) of PCs in popliteal LNs at day 7. Data in (B) and (E) were analyzed as detailed in A. Data in (D) and (E) were analyzed as detailed in Figure 1A.

In **(A-B)** and **(D-E)** n = 9 mice per group were analyzed. Data were combined from three independent experiments. In **(C)** n = 6 mice per group were analyzed. Data were combined from two independent experiments. Data are shown as mean ± SEM and each point represents an individual mouse. One-way-ANOVA with Bonferroni correction or unpaired two-tailed Mann-Whitney U tests was conducted according to the distribution of the data. * $p \leq 0.05$, ** $p \leq 0.01$, *** $p \leq 0.001$, **** $p \leq 0.0001$.

Figure S2. Immunization with SARS-CoV-2 mRNA vaccines elicit full S-specific GC B cell responses. Related to Figure 2. For panels **(A-D)** and **(G-L)** mice were i.m. immunized with SARS-CoV-2 mRNA vaccines, Luc mRNA control or rRBD-AddaVax as previously described. For panels **(E-F)** mice were immunized i.m. with 20 μg of RBD mRNA or 20 μg of rRBD-AddaVax. **(A-F)** Data were analyzed at day 7. **(G-L)** GC B cells from draining inguinal LNs were measured 7, 14, 21 or 28 days post immunization. **(A)** Representative contour plots showing full S-specific GC B cells in the different study groups, defined as live, dump$^-$, CD19$^+$FAS$^+$GL7$^+$full S-PE$^+$full S-AF647$^+$ cells. **(B-F)** Frequency (left) and absolute numbers (right) of: **(B)** full S-specific GC B cells in inguinal LNs (as defined in A); **(C)** RBD-specific GC B cells in popliteal LNs, as defined in Figure 2A. **(D)** Full S-specific GC B cells in popliteal LNs (as explained in A); **(E)** GC B cells in inguinal LNs (as defined in Figure 1A); **(F)** RBD-specific GC B cells in inguinal LNs (As defined in Figure 2A). **(G-L)** Kinetics of: **(G)** absolute numbers of full S-specific GC B cells in inguinal LNs; **(H)** GC B cell frequencies in inguinal LNs; **(I)** frequency of RBD-specific

GC B cells in inguinal LNs, **(J)** total lymphocyte numbers in inguinal LNs; **(K)** absolute numbers of GC B cells in inguinal LNs of rRBD-AddaVax immunized mice; **(L)** absolute numbers of RBD-specific GC B cells in inguinal LNs of rRBD-AddaVax immunized mice. For kinetic plots, day 0 represents the average of 18 naive mice. For **(K-L)**, red dotted line represents the mean of RBD mRNA vaccinated mice at designated timepoints.

In **(A-C)**, n = 8 mice per group were analyzed for RBD mRNA group, and n = 9 mice per group for all other groups were analyzed. Data are combined from three independent experiments. In **(D)** n = 9 mice per group were analyzed. Data are combined from three independent experiments. In **(E)** and **(F)**, n = 8 mice per group were analyzed. Data are combined from two independent experiments. In **(B-F),** each point represents an individual mouse. In **(G)** and **(I)**, the same number of mice per group were analyzed as in **(A-C)** for days 7 and 14. n = 10 mice per group were analyzed and data are combined from two independent experiments at day 28. In (**H)** and **(J)**, the same number of mice per group were analyzed as in **(D)** for days 7 and 14. n = 10 mice per group were analyzed and data are combined from two independent experiments at day 28. In **(K)** and **(L)**, n = 9 mice per group were analyzed for days 7 and 14. n = 6 mice per group were analyzed for day 21. For kinetic plots **(G-J)**, statistics were calculated versus Luc mRNA group. Data are graphed as mean ± SEM. One-way-ANOVA with Bonferroni correction or unpaired two-tailed Mann-Whitney U tests was conducted according to the distribution of the data. * $p \leq 0.05$, ** $p \leq 0.01$, *** $p \leq 0.001$, **** $p \leq 0.0001$

Figure S3. SARS-CoV-2 mRNA vaccines promote the generation of full S-specific MBC precursors and bona fide MBCs. Related to Figure 3. Mice were i.m. immunized with SARS-CoV-2 mRNA vaccines, Luc mRNA control or rRBD-AddaVax as previously described. **(A)** Inguinal LNs were analyzed 7 days post immunization. Frequency (left) and absolute numbers (right) of full S-specific MBC precursors. **(B-I)** Spleens were analyzed 60 days post immunization. **(B)** Representative contour plots of full S-specific $IgG1^+$ MBCs, pre-gated on singlets, live, $dump^-$, and $CD19^+B220^+IgD^-FAS^-CD38^+IgG1^+$ cells. **(C)** Frequency (left) and absolute numbers (right) of full S-specific $IgG1^+$ MBCs as explained in (B). **(D)** Representative flow cytometry analysis of full S-specific $IgG2a/2b^+$ MBCs, pre-gated on singlets, live, $dump^-$, and $CD19^+B220^+IgD^-FAS^-CD38^+IgG2a/2b^+$ cells. **(E)** Frequency (left) and absolute numbers (right) of full S-specific $IgG2a/2b^+$ MBCs as explained in (D). **(F, H)** Representative contour plots of: **(F)** RBD-specific

and **(H)** full S-specific IgM^+ MBCs, pre-gated on singlets, live, $dump^-$, and $CD19^+B220^+IgD^-FAS^-CD38^+IgM^+$ cells. **(G, I)** Frequency (left) and absolute numbers (right) of: **(G)** RBD-specific IgM^+ and **(I)** full S-specific IgM^+ MBCs (as explained in F and H, respectively).

In **(A-I)**, n = 8 mice per group were analyzed for RBD mRNA group, and n = 9 mice per group for all other groups were analyzed. Data are combined from three independent experiments. In **(A)**, **(C)**, **(E)**, **(G)** and **(I)** data are shown as mean ± SEM and each point represents an individual mouse. One-way-ANOVA with Bonferroni correction or unpaired two-tailed Mann-Whitney U tests was conducted according to the distribution of the data. * $p \leq 0.05$, ** $p \leq 0.01$, *** $p \leq 0.001$, **** $p \leq 0.0001$.

Figure S4. SARS-CoV-2 mRNA immunized animals exhibit elevated SARS-CoV-2-specific Ab titers and nAbs. Related to Figure 4. Mice were i.m. immunized with SARS-CoV-2 mRNA vaccines, Luc mRNA control or rRBD-AddaVax as previously described. **(A-D)** Serum was collected at 14 (left), 28 (middle) and 60 (right) days post immunization. SARS-CoV-2 specific Ab titers were determined by ELISA. RBD-specific: (**A)** IgG; **(B)** IgG1; **(C)** IgG2a and **(D)** IgG2b responses are plotted. **(E)** Bone marrow (BM) was collected at day 60 post immunization. Quantification of full S-specific IgG^+ ASC in BM was determined by ELISPOT. **(F-J)** Spearman correlations of: **(F)** RBD-specific IgG titers and nAb levels (MEC) at 60 days post immunization; **(G)** RBD-specific IgG^+ ASC and nAb levels (MEC) at 60 days post immunization; **(H)** inguinal LN GC B cells (cells x 10^5) and nAb levels (MEC) at 14 days post immunization; **(I)** RBD-specific GC B cells (cells x 10^5) from inguinal LNs and nAb levels (MEC) at 14 days post immunization; and **(J)** full S-specific GC B cells (cells x 10^5) from inguinal LNs and nAb levels (MEC) at 14 days post immunization.

In **(A-D)** and **(F-H)** n = 9 mice per group were analyzed. Data are combined from three independent experiments. In **(E)** n = 6 mice per group were analyzed. Data are combined from two independent experiments. In **(I-J)** n = 8 mice per group were analyzed for RBD mRNA group, and n = 9 mice per all other groups were analyzed. Data are combined from three independent experiments. In **(A-D)** data is shown as geometric mean ± geometric SD. In **(E)** mean ± SEM are shown. In all graphs, each point represents an individual mouse. One-way-ANOVA with Bonferroni correction or unpaired two-tailed Mann-Whitney U tests was conducted according to the distribution of the data. * $p \leq 0.05$, ** $p \leq 0.01$, *** $p \leq 0.001$, **** $p \leq 0.0001$

Figure S5. Tfh cells are increased in mRNA-vaccinated animals. Related to Figure 5. Mice were i.m. immunized with SARS-CoV-2 mRNA vaccines, Luc mRNA control or rRBD-AddaVax as previously described. Naive mice were also included as control. Tfh cells from: **(A-E)** inguinal or pooled inguinal and **(F)** popliteal LNs were evaluated at different time points. **(A)** Representative contour plots of Tfh cell defined as $CXCR5^{+}PD\text{-}1^{+}$ cells pre-gated on singlets, live, and $B220^{-}CD4^{+}CD44^{hi}CD62L^{-}$ populations at 7 days post immunization. **(B)** Frequency (left) and absolute numbers (right) of Tfh cells as defined in (A). **(C)** Frequency (left) and absolute numbers (right) of Tfh cells defined as live, $B220^{-}CD4^{+}CD44^{hi}CD62L^{-}CXCR5^{+}Bcl\text{-}6^{+}$ at 21 days post immunization. **(D-E)** Spearman correlations of: **(D)** GC B cells (cells x 10^5) and $CXCR5^{+}PD\text{-}1^{+}$ Tfh cells (cells x 10^5) at 7 days post immunization and **(E)** $CXCR5^{+}PD\text{-}1^{+}$ Tfh cells (cells x 10^5) and nAb levels at 14 days post immunization. **(F)** Representative gating strategy defining Tfh cells in ICS experiments upon SARS-CoV-2 peptide pool stimulation at 7 days post immunization. In **(A-B)** and **(D-E)** n = 8 mice per group were analyzed for RBD mRNA group, and n = 9 mice per group for all other groups were analyzed. Data are combined from three independent experiments. In **(C)** n = 6 mice per group were analyzed. Data are combined from two independent experiments. In **(B-C)** data is graphed as mean ± SEM. In **(B-E)** each point represents an individual mouse. One-way-ANOVA with Bonferroni correction or unpaired two-tailed Mann-Whitney U tests was conducted according to the distribution of the data. * $p \leq 0.05$, ** $p \leq 0.01$, *** $p \leq 0.001$, **** $p \leq 0.0001$

Figure S6. Features of Tfh cells induced by SARS-CoV-2 vaccines. Related to Figure 6. Balb/c (A-E) and (L-M) or C57BL/6J mice (F-K) were i.m. immunized with SARS-CoV-2 mRNA or rRBD-AddaVax as previously described and Tfh cells were evaluated at 7 days post immunization. **(A)** Representative gating strategy defining Tfh cells ($CXCR5^{+}PD\text{-}1^{+}$) by flow cytometry intracellular staining after PMA/ionomycin activation in inguinal LNs. **(B, D)** Representative flow cytometry analysis of: **(B)** IFN-γ^{+} or **(D)** IL-4^{+} Tfh cells ($CXCR5^{+}PD\text{-}1^{+}$) in pooled inguinal and popliteal LNs of the different study groups upon SARS-CoV-2 peptide stimulation. Cells were pre-gated on singlets, live, and $CD4^{+}B220^{-}CD44^{lo}$ populations. **(C, E)** Frequency of: **(C)** IFN-γ^{+} or **(E)** IL-4^{+} producing Tfh cells analyzed as detailed in (B) and (D), respectively. **(F-G)** In C57BL/6J mice, frequency of **(F)** IFN-γ^{+} or **(G)** IL-4^{+} producing Tfh cells analyzed as detailed in

(B) and (D), respectively. **(H)** Ratio of IL-4$^+$ to IFN-γ$^+$ producing Tfh cells in C57BL/6J mice. **(I-K)** In inguinal LNs of C57BL/6J mice, absolute numbers of: **(I)** GC B cells defined as live dump$^-$, CD19$^+$FAS$^+$GL7$^+$; **(J)** RBD$^+$ GC B cells defined as live dump$^-$, CD19$^+$FAS$^+$GL7$^+$RBD-AF647$^+$RBD-PE$^+$; and **(K)** Tfh cells defined as live $^+$CD4$^+$B220$^-$CD44^{hi}CD62L$^-$CXCR5$^+$Bcl-6$^+$. **(L)** Mean Fluorescence Intensity (MFI) of Bcl-6 on Tfh cells (CXCR5$^+$PD-1$^+$) in inguinal LNs. **(M)** Spearman correlation of ICOS MFI and the frequency of Tfh cells (CXCR5$^+$Bcl-6$^+$) in pooled inguinal and popliteal LNs.

In **(A)** and **(L)** n = 9 mice per group were analyzed. Data were combined from three independent experiments. In **(B-E)** n = 10 mice per group were analyzed. Data were combined from four independent experiments. In **(F-K)** n = 8 mice per group were analyzed. Data were combined from two independent experiments. In **(M)** n = 8 mice per group across two independent experiments. For **(C)**, **(E)**, and **(F-K)** data are graphed as mean ± SEM and each point represents an individual mouse. One-way-ANOVA with Bonferroni correction or unpaired two-tailed Mann-Whitney U tests was conducted according to the distribution of the data. * $p \leq 0.05$, ** $p \leq 0.01$, *** $p \leq 0.001$, **** $p \leq 0.0001$

Figure S7. Secondary Tfh cell differentiation following a booster immunization. Related to Figure 7. Mice were i.m. immunized with Luc mRNA control, RBD mRNA, or rRBD-AddaVax as previously described. After 28 days, all groups received a second immunization with the same vaccine. Serum and draining inguinal LNs were analyzed 10 days following the second immunization. **(A)** Frequencies (left) and absolute numbers (right) of Tfh cells defined as live CD4$^+$B220$^-$CD44^{hi}CD62L$^-$CXCR5$^+$Bcl-6$^+$. **(B)** Spearman correlation analysis of absolute numbers of GC B cells and nAb IC_{50}. In **(A-B)** n = 7 mice per group were analyzed. Data were combined from two independent experiments. Data are graphed as Mean ± SEM and each point represents an individual mouse. Unpaired two-tailed Mann-Whitney U tests was conducted according to the distribution of the data. * $p \leq 0.05$, ** $p \leq 0.01$, *** $p \leq 0.001$, **** $p \leq 0.0001$.